First US-Europe Air Transportation Research and Development Symposium (ATRDS2025)

Including intent in detect-and-avoid systems for remotely piloted aircraft systems

Sybert Stroeve, Mirco Kroon
Royal Netherlands Aerospace Centre NLR
Amsterdam, The Netherlands
sybert.stroeve@nlr.nl; mirco.kroon@nlr.nl

***Abstract*—Current standards for detect-and-avoid (DAA) systems of remotely piloted aircraft systems (RPAS) use state data like (relative) position and speed for the provision of guidance to remain well clear (RWC) with air traffic. They do not use intent data for planned route towards a destination. This paper proposes an intent-based DAA system that uses an A* path planning approach. The performance of this A* DAA system is compared with the ACAS Xu standard for a set of horizontal encounters between RPAS pairs. This comparison is done for deterministic and stochastic encounter-scenarios, which account for sensor errors and variation in remote pilot performance. The results show that in the ACAS Xu scenarios the aircraft can attain livelock conditions that prevent them from reaching their destination. Also, in these encounter-scenarios often loss of DAA well clear (LDWC) conditions occur, and they are sensitive for sensor errors and closed-loop delays. The simulation results of the A* DAA encounter-scenarios are without livelock or LDWC conditions and the variations due to sensor errors and closed-loop delays are limited. They show that the intent-based A* DAA system is a promising approach for more effective DAA.**

Keywords - remotely piloted aircraft system; detect-and-avoid system; A* path planning; ACAS Xu; remain well clear

I. INTRODUCTION

A detect-and-avoid (DAA) system supports a remote pilot (RP) of a remotely piloted aircraft (RPA) to observe and avoid nearby air traffic or other hazards using sensor and guidance technology. While such other hazards relating to terrain and obstacles, dangerous meteorological conditions, ground operations, wake turbulence, etc., would need to be handled appropriately in support of airspace integration [1], current DAA systems predominantly focus on conflicting traffic. This is also the focus of this paper. In general, such a DAA system can have a remain well clear (RWC) and a collision avoidance (CA) function. The RWC function supports detection and analysis of potential conflicting traffic and provides flight path guidance to the RP to prevent the conflict developing into a collision hazard [2]. In combination with air traffic control (ATC), the RWC function supports separation provision in air traffic conflict management [1]. The CA function provides last-resort resolution advisories (RAs) to the RP to avoid physical contact between the aircraft. The RWC and CA functions may use multiple degrees of freedom (DOF) in their guidance and advisories, in particular for manoeuvring horizontally, vertically, or changing speed. It is up to the RP, often in coordination with ATC, to decide on and implement an appropriate control strategy given the DAA output. In case of non-response by the RP to RAs by the CA functionality, there may be automatic responses by the flight management system (FMS) of the RPA.

A number of DAA standards have been published. RTCA published minimum operational performance standards (MOPS) for DAA [2], providing detailed equipment performance requirements, test procedures, and operational services and environment description (OSED) for larger (above 55 pounds) RPA mostly operating in airspace classes D, E, and G. It also describes the Detect and Avoid Alerting Logic for Unmanned Aircraft System (DAIDALUS) as a reference implementation. DAIDALUS algorithms and software have been developed by NASA and include logic for detection manoeuvre guidance, and alerting [3]; surveillance data processing is not included. It is a rule-based system that can be tuned to specific aircraft or operation characteristics by a set of configuration parameters. EUROCAE published a minimum aviation system performance standard (MASPS) for DAA [4], specifying characteristics of a DAA system as a basis for more detailed MOPS. As part of the FAA sponsored ACAS X programme, ACAS Xu was developed as a DAA system for remotely piloted aircraft systems (RPAS) [5]. ACAS Xu is a fully specified system (EUROCAE ED-275 [6] / RTCA DO-386), including surveillance filtering, conflict detection, manoeuvre guidance and alerting. The threat resolution module (TRM) of ACAS Xu is based on partially observable Markov decision process (POMDP) models and objective functions, which have been solved by a dynamic programming (DP) approach to calculate a Q-function representing the value gained for taking an action in the current state. In ACAS Xu the Q-functions are represented as lookup tables with a total size of 5 GB. The RWC guidance provided by ACAS Xu is based on a rollout approach [7], which uses the POMDP-based cost tables to infer an increase in collision risk in relation to DAA alert timing requirements.

In all above DAA standards and supporting studies [2-6] a variety of state data is used as input of DAA systems. This may include state data from the ownship, such as its horizontal position and speed, altitude and vertical rate, heading and airspeed, as well as uncertainty metrics for such state data. It may include data from nearby traffic (intruders) like slant range and rate, horizontal position and speed, relative bearing angle, altitude and vertical rate, as well as uncertainty metrics. For the provision of RAs by the CA functionality, a DAA system may

This work is supported by the Horizon Europe EIC project SymAware (101070802).

use coordination messages to achieve suitable complementary advisories with another aircraft (e.g. one climbs, other descends). No DAA system coordination is used for the RWC functionality.

A DAA system is part of a sociotechnical RPAS, which also includes navigation and surveillance systems, command & control (C2) links, a remote pilot station (RPS), and importantly the RP, who controls the aircraft and responds to DAA guidance and advisories. In evaluation of the effectiveness of DAA systems, the performance of all elements of the sociotechnical RPAS should be accounted for systemically. This includes sensor data and errors, aircraft performance, delays, and RP performance. An agent-based modelling and simulation environment for evaluation of ACAS Xu, which uses such systemic perspective, was described in [8]. A key finding in that paper is that livelock conditions can exist in ACAS Xu supported RPAS operations, where RPA attain continuing fluctuations away from an intruder and back to their course without reaching their destination. It was recognized that current DAA systems only provide guidance and advisories for avoiding other traffic, which are based on state data. However, they do not take into account planned routes or destinations (intent data) of the RPA in the guidance provision. In operations such intent data is typically available to RPs, ATC and in the flight management system, but it is not part of DAA standards. This may lead to suboptimal or problematic DAA guidance and advisories.

As a way forward this paper presents an intent-based DAA system for horizontal manoeuvring and its performance is evaluated for several encounters, sensor errors and RP performance variability in comparison with the state-based ACAS Xu system. The intent-based DAA system extends an A* path planning conflict resolution approach of [9]. Section II presents the intent-based A* DAA approach. Section III describes the evaluation approach for comparison of ACAS Xu and the A* DAA systems. Section IV presents illustrative simulation runs and statistics for ACAS Xu and A* DAA. Section V discusses the findings and their implications.

II. INTENT-BASED A* DAA APPROACH

A. *Intent-based DAA control architecture*

A system diagram of a pair of aircraft with intent-based DAA systems is shown in Figure 1. Aircraft *i,j* have states $\mathbf{x}_i, \mathbf{x}_j$, which encompass the position and speed of the aircraft. Ownship state estimation by the aircraft lead to state estimates $\hat{\mathbf{x}}_i, \hat{\mathbf{x}}_j$, which include errors. In this study, state estimates are shared instantaneously between the aircraft in an encounter, but (possibly stochastic) delays are incorporated in the implementation of DAA guidance. It is assumed that conflict detection is performed based on the shared state estimates and possibly on intended future waypoints. State-based conflict detection uses a linear future projection of the states to decide on the conflict risk within a suitable timeframe. If a conflict is detected by aircraft *i* a signal $\kappa_{i,j}^{CD}$ concerning the conflict detection is sent to all aircraft in the encounter-scenario; it is also sent to the (nearby) aircraft that are not detected to be in conflict (yet). The conflict detection algorithm is provided later in this section.

Upon detection of a conflict all aircraft in the encounter-scenario instantaneously share their planned routes $\bar{\mathbf{X}}_i, \bar{\mathbf{X}}_j$, which consist of a series of future waypoints. These initial planned routes are the start point of an intent-based conflict resolution approach. This conflict resolution assumes the existence of a central agency that plans the paths of all aircraft in the encounter. This central agency can be one of the aircraft in the encounter-scenario. Given the assumption that all aircraft have the same information (state estimates and planned routes) at the same time, the outcome of the conflict resolution does not depend on the aircraft chosen as central agent. The path planning leads to updated planned routes $\bar{\mathbf{X}}_i, \bar{\mathbf{X}}_j$, which can alternatively be represented by a series of planned rates of turn $\bar{\boldsymbol{\omega}}_i, \bar{\boldsymbol{\omega}}_j$. Upon reaching a solution the central agency informs each aircraft about the routes planned to resolve the conflict.

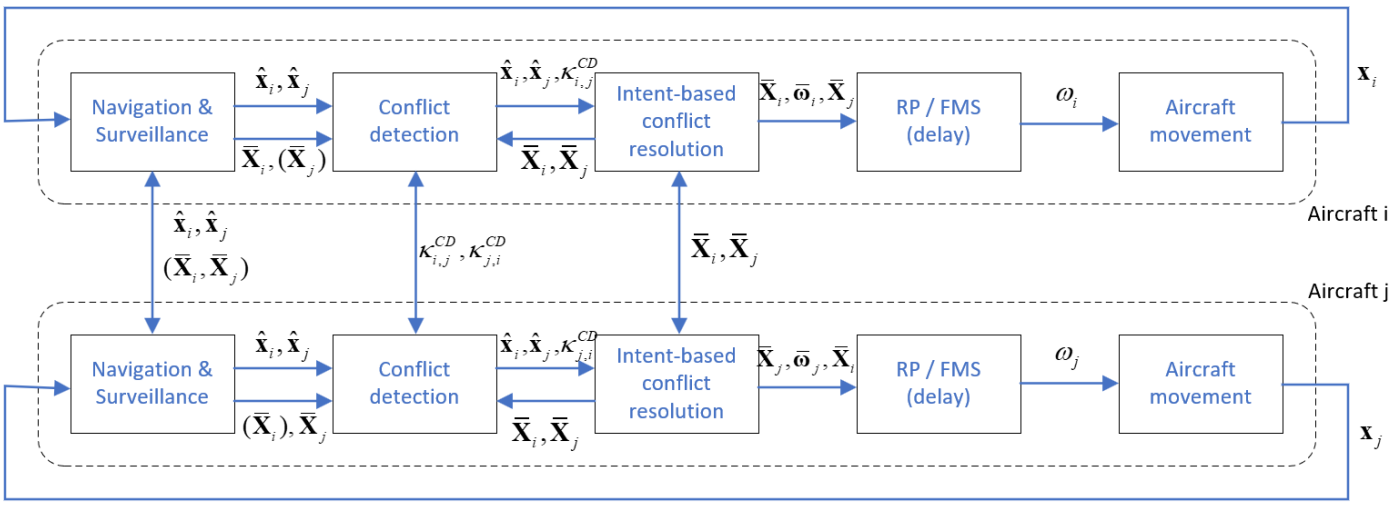

Figure 1. System diagram for an intent-based DAA control architecture.

Given a planned route the remote pilot or the FMS in the case of automatic response turns the aircraft in the horizontal plane so as to follow the planned route / rates of turn. The manoeuvring is assumed to be done with a particular closed-loop response delay.

B. Conflict risk costs

As a basis for the conflict detection and resolution a conflict risk cost function is defined, which assigns costs to close future approaches while accounting for uncertainty in the future trajectories of the aircraft. This is an extension of work in [9].

It is assumed that there are prediction errors in the position of each aircraft, which consist of zero-mean normally distributed along-track errors with standard deviation (SD) σ_i^a and a cross-track errors with SD σ_i^c, such that the covariance matrix in a heading-aligned coordinate system is

$$\mathbf{K}_i = \begin{pmatrix} (\sigma_i^a)^2 & 0 \\ 0 & (\sigma_i^c)^2 \end{pmatrix} \quad (1)$$

Using a heading-based rotation matrix $\mathbf{R}_i$ the heading-aligned covariance matrix is transformed to the reference coordinate system:

$$\mathbf{Q}_i = \mathbf{R}_i \mathbf{K}_i \mathbf{R}_i^T \quad (2)$$

In this way for an aircraft pair (*i,j)* the covariance matrices $\mathbf{Q}_i, \mathbf{Q}_j$ are attained. Assuming that cross-correlations between position errors are zero, the covariance matrix of the uncertainty in the distance between the aircraft is $\mathbf{Q}_{ij} = \mathbf{Q}_i + \mathbf{Q}_j$. Now a conflict risk cost for the planned positions $\overline{\mathbf{x}}_i, \overline{\mathbf{x}}_j$ is defined as being proportional to the probability density of the distance between the aircraft:

$$c_{i,j}^{CR} = k_1 \exp\left(-\tfrac{1}{2}(\overline{\mathbf{x}}_i - \overline{\mathbf{x}}_j)^T \mathbf{Q}_{ij}^{-1} (\overline{\mathbf{x}}_i - \overline{\mathbf{x}}_j)\right) \quad (3)$$

where k_1 is a tuning parameter. To account for multiple intruders, the total costs of the ownship is the sum of the costs with respect to all intruders:

$$c_i^{CR} = \sum_{j \neq i} c_{i,j}^{CR} \quad (4)$$

An illustration of the conflict risk costs between a pair of aircraft is shown in Figure 2. Here both aircraft have prediction errors with σ_i^a = 600 m and σ_i^c = 400 m, k_1 = 3, and the aircraft have relative courses of 0, 45, 90, or 135 deg. It shows that the shape as well as the principal axis of the distribution depend on the relative course.

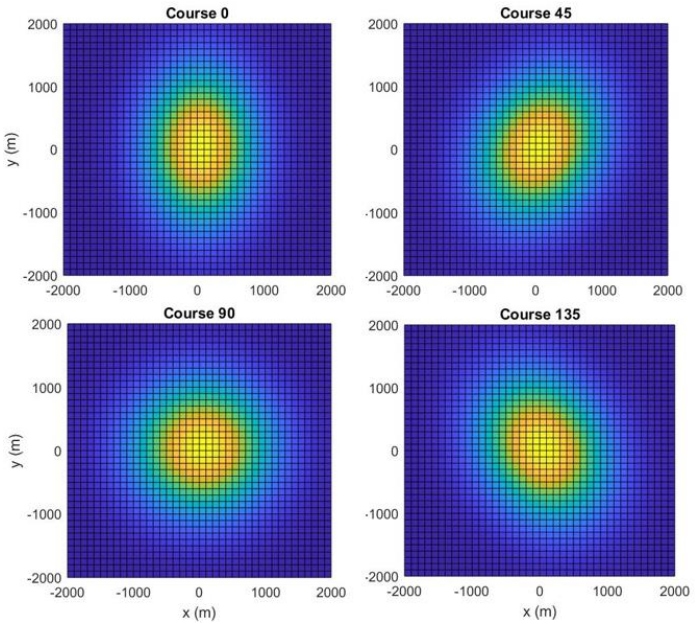

Figure 2. Illustration of a conflict risk costs between two aircraft, where the relative course is 0, 45, 90, or 135 degrees.

C. Conflict detection and route adherence check

The conflict detection is based on the integrated conflict risk costs for an aircraft pair *i,j* over a time horizon τ^{CD} (set to a value 180 s):

$$c_{i,j}^{ICR} = \int_t^{t+\tau^{CD}} c_{i,j}^{CR} \quad (5)$$

A conflict is detected if the integrated costs for a pair is equal or larger than a threshold θ_i^{CD} (set to a value 5):

$$\kappa_{i,j}^{CD} \equiv (c_{i,j}^{ICR} \geq \theta_i^{CD}) \quad (6)$$

Furthermore, the DAA system uses a route adherence check, which evaluates for each aircraft in the encounter-scenario whether the observed state is in accordance with its planned state:

$$\kappa_i^{RA} \equiv (\left|\hat{\mathbf{x}}_i - \overline{\mathbf{x}}_i\right| \leq \theta_i^d) \wedge (\left|\hat{\varphi}_i - \overline{\varphi}_i\right| \leq \theta_i^h) \quad (7)$$

where $\hat{\mathbf{x}}_i$ is the current position estimate, $\overline{\mathbf{x}}_i$ is the associated planned position, θ_i^d is a distance deviation threshold, $\hat{\varphi}_i$ is the current heading estimate, $\overline{\varphi}_i$ is the associated planned heading, and θ_i^h is a heading deviation threshold.

If either a conflict is detected or there is a route adherence failure for any of the aircraft in an encounter-scenario, then the A* conflict resolution step is initiated for all aircraft in the encounter-scenario, as explained next.

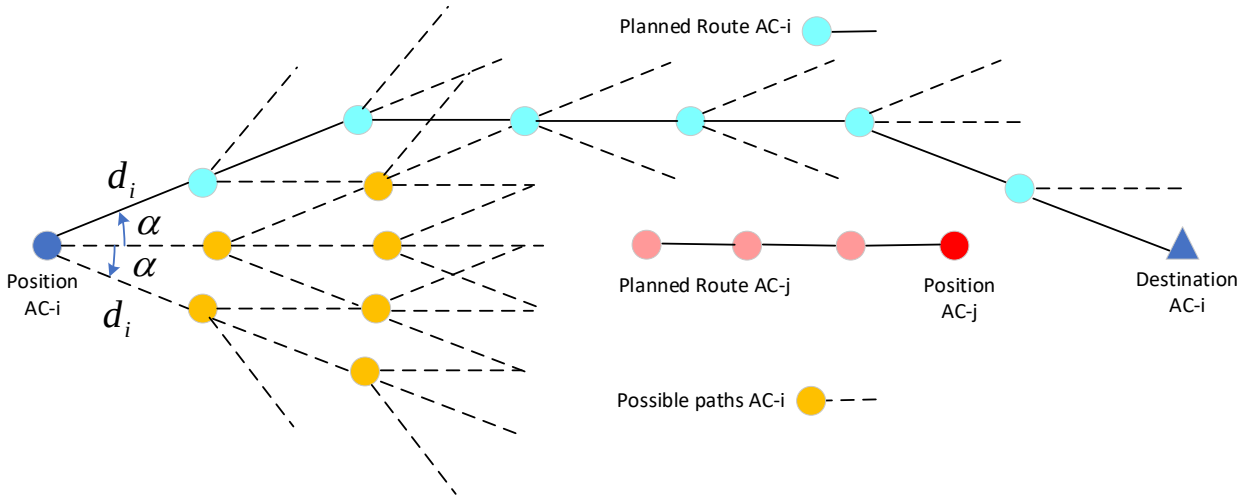

Figure 3. Illustration of path planning for AC-i from a start to a destination, while evading the planned route of AC-j.

*D. Intent-based conflict resolution using A**

The conflict resolution approach is formulated as a path planning problem, which minimizes the total cost of a flight path towards a goal by considering both the distance and the total conflict risk cost along the path. This is done using the A* path solving algorithm [10]. Since A* works using a graph of nodes and edges, flight paths need to be represented as such, as illustrated in Figure 3.

Using a discrete time step t_d the flight path of aircraft *i* flying at a constant speed v_i is represented by a set of nodes that are connected by edges of length $d_i = v_i t_d$. Neighbouring nodes are added to each node, which represent possible turns in the route planning. In this study three neighbours per node have been applied, representing a left or right turn over an angle α, or going straight. For the results in this study, we used t_d =10 s and α =20 deg.

The A* search algorithm is an informed best-first search algorithm, which uses an evaluation function

$$f(n) = g(n) + h(n) \tag{8}$$

where $g(n)$ is the path cost from the initial state to node n, and $h(n)$ is a heuristic function for the estimated cost of the shortest path from n to a goal state [10]. The A* algorithm is complete, meaning that it is guaranteed to find a solution when there is one. A* is cost-optimal (i.e. it finds a solution with the lowest costs) if the heuristic function is admissible. An admissible heuristic means that it never overestimates the cost to reach a goal.

In addition to the conflict risk costs c_i^{CR} defined in Eq.(4) we define flight trajectory element costs c_i^{FT} for the costs of an aircraft to traverse during a time t_d to a next node in the network. The search for an optimal path given these costs can be achieved by the following path costs and heuristic function:

$$\begin{aligned} g_i(n) &= g_i(n-1) + c_i^{FT} + c_i^{CR} \\ h_i(n) &= k_2 c_i^{FT} \frac{\left\| \bar{\mathbf{x}}_i(n) - \bar{\mathbf{x}}_i(G) \right\|}{d_i} \end{aligned} \tag{9}$$

Herein the path cost $g_i(n)$ is increased by the flight trajectory element cost plus the total conflict risk. The positive factor k_1 in Eq.(3) allows to provide more emphasis on the conflict risk, in particular larger values lead to more risk adverse paths. The heuristic function $h_i(n)$ determines the minimum flight trajectory costs by multiplying the number of steps needed to pass the distance between the aircraft position at the current node with respect to its goal G by the flight trajectory element cost, and it weights this value with a positive factor k_2. If $k_2 \leq 1$ then the heuristic is admissible, thus assuring the search to be cost-optimal. However, setting $k_2 > 1$ may reduce the solution space and thus accelerate the search, while still providing acceptable results. For the results in this paper, we used k_1 =3, k_2 =1, and c_i^{FT} =1 for each aircraft.

Above A* path planning approach finds an optimal flight trajectory for a single flight given that the intruders that need to be avoided do not adapt their trajectories. A next step is to achieve a multi-agent optimization that adapts the trajectories of multiple aircraft. This is done by a series of ordered single-agent A* optimizations, where one the aircraft is optimized at the time given fixed trajectories of other aircraft. This process starts with the determination of an order in the sequence of aircraft. For this order the trajectory of each aircraft is adapted using A*, while the trajectories of other aircraft are fixed. The

iterations continue until the differences in the solutions are sufficiently small.

It was shown in [9] that the sum of the path costs of all aircraft in the multi-agent system is monotonically decreasing in iterations of such series of ordered single-agent A* optimizations. The attained total costs and the particular planned trajectories of the multi-agent system depend on the settings of the conflict risk costs and the flight trajectory element costs, as well as on the ordering of the aircraft in the sequence of A* optimizations. For the results of two-aircraft encounters shown in this paper, aircraft coming from the right are placed last in the sequence, so as to stimulate the other aircraft to manoeuvre away from the aircraft having right-of-way in the horizontal encounter [2]. In encounters with more than two aircraft the order follows the aircraft numbering.

III. EVALUATION APPROACH

A. Encounters

For comparison of the A* DAA approach with ACAS Xu, a limited set of eight encounters between RPA pairs (AC1, AC2) is used in this study. The planned aircraft trajectories are straight, remain in a horizontal plane at an altitude of 8000 ft (2438 m), and have constant speed. There is no wind. All planned aircraft trajectories in an encounter have an HMD of 0 m. The duration of an encounter is from 300 s before to 300 s after the closest point of approach (CPA). The heading of AC1 is always 0 deg, while the heading of AC2 may be 45, 90, 135, or 180 deg. The speed of AC1 is always 120 kt (61.7 m/s), while the speed of AC2 may be 120 kt or 140 kt (72.0 m/s).

In addition to these two-aircraft encounters the performance of the A* DAA approach is evaluated for a set of four encounters involving three aircraft (AC1, AC2, AC3) at 8000 ft for a duration of 10 minutes, and with an HMD of 0 m. The heading of AC1, 2 and 3 are either 0, 120, 240 deg (resp.), or 0, 90, 270 deg. The speeds of AC1, 2 and 3 are all 120 kt, or 120, 100, 140 kt (resp.).

B. Scenarios

1) DAA equipment level

The DAA equipment level of a scenario may be full, i.e. all aircraft are equipped with the same DAA system and provide RWC guidance, or it may be partial, where AC1 is not equipped and does not provide RWC guidance.

2) RP performance

The RP responds to horizontal RWC guidance only; thus the aircraft remain in the horizontal plane. The RP always responds and exactly follows the RWC guidance; there is no bias with respect to RWC bands or advised heading. There is a closed-loop response delay, concerning the time between the provision of (updated) RWC guidance and the time that the aircraft starts to manoeuvre in line with the guidance. The following conditions for the closed-loop delay are discerned:

- *Auto.* This represents the situation of an automatic response by the FMS of the unmanned aircraft (without any interaction by a RP). For this a constant delay of 1 s is set for each aircraft in the encounter-scenario.
- *Quick.* This represents the situation of quick responses by a RP, including the time for downlink, swift reaction of the RP, and uplink. For this a constant delay of 4 s is set for each aircraft in the encounter-scenario.
- *Slow.* This represents the situation of slow(er) responses by a RP, including the time for downlink, reaction of the RP who possibly interacts with ATC, and uplink. For this a constant delay of 12 s is set for each aircraft in the encounter-scenario.
- *Stochastic.* A constant delay time chosen from a lognormal distribution at the start of the encounter-scenario for each aircraft separately. The delay has a mean of 4 s and a SD of 2.5 s (implying that the probability of a delay less than 1 s is 0.017 and the probability of a delay more than 12 s is 0.014).

3) Sensors

The position and speed of an ownship are estimated using a Global Navigation Satellite System (GNSS). This state estimate may contain errors. The position and velocity estimate errors are modelled by first-order autoregressive processes with normally distributed noise (SD is 37.8 m or 4.08 m/s; autocorrelation factors are 0.997). The main source for the altitude estimation of an ownship is based on pressure altitude. The altitude estimates are assumed to be without error in the scenario, since the focus is on horizontal manoeuvring only. The state estimate of an ownship is shared with an intruder using a communication link (ADS-B: automatic dependent surveillance broadcast). This communication link is assumed to be without delay of error. The ownship state estimation and ADS-B is used by both ACAS Xu and A* DAA.

An aircraft can estimate the slant range (distance) and bearing angle with respect to an intruder by transponder-based measurements. These measurements may contain errors. The slant range error and bearing error are modelled by first-order autoregressive processes with normally distributed noise (SD is 41.0 m or 12 deg; autocorrelation factors are 0.997). These intruder measurements are used by ACAS Xu only.

C. Simulation environments and settings

The ACAS Xu supported encounter-scenarios are simulated using the Collision Avoidance Validation and Evaluation Tool (CAVEAT). It is based on a stochastic dynamic agent-based modelling and simulation approach [11, 12] and supports retrospective and prospective analysis of encounter-scenarios with DAA and airborne collision avoidance systems (ACAS), including TCAS II, ACAS Xa, and ACAS Xu. The C++ based CAVEAT software was developed for EUROCONTROL by NLR and everis/NTT-Data. The software of ACAS Xu consists of the validated Julia libraries as provided in the MOPS [13].

The A* DAA supported encounter-scenarios are simulated in dedicated Java software that was developed by NLR for the A* DAA algorithms, as well as the representation of the encounter-scenarios.

There are six deterministic scenarios for both DAA systems, representing the combinations of the three fixed

closed-loop delays, and full or partial DAA equipment levels. Each scenario is simulated for the set of encounters.

There are ten stochastic scenarios for both DAA systems, representing sensor errors in combination with fixed or stochastic closed-loop delays, and full or partial DAA equipment levels, as well as stochastic delays without sensor errors. Each stochastic scenario is simulated by 100 MC simulation runs per encounter.

D. *Evaluation metrics*

The following metrics are used for evaluation of DAA systems in encounter-scenarios.

- *Loss of DAA Well Clear (LDWC) percentage.* A LDWC has been defined to occur for en-route cooperative aircraft [2] if the following conditions all apply: (1) the projected horizontal miss distance (assuming constant speed) is less or equal than 4000 ft (1219 m), (2) the so-called modified tau (for large range approximately the time to pass the range) is less or equal than 35 s, and (3) the vertical separation is less or equal than 450 ft. The LDWC percentage is the part of the runs where an LDWC occurred.
- *NMAC percentage.* In ACAS validation studies traditionally near mid-air collision (NMAC) events are used as a key metric. It is defined as VMD being less than 100 ft (30.5 m) and HMD being less than 500 ft (152.4 m). The NMAC percentage is the part of the runs where an NMAC occurred.
- *Horizontal Miss Distance (HMD).* The HMD is the distance in the horizontal plane between a pair of aircraft at CPA. The mean and standard deviation of the HMD in the runs of a scenario are gathered.
- *Additional flight distance (AFD).* As a result of the DAA guidance the trajectory is adapted and additional distance is traversed. The horizontal distance for each aircraft is determined by the integrals of the traversed distance for the original trajectory and the modified trajectory. The additional distance of an aircraft is the difference of the traversed distances plus the distance between the points at the end of the original and modified trajectories. The additional distance in a run is the sum of the additional distances. The mean and standard deviation of the AFD in the runs of a scenario are gathered.

IV. RESULTS

A. *ACAS Xu simulation runs for two-aircraft encounters*

Firstly, a number of illustrative simulation runs are shown for the RPAS dynamics in encounters where one or both systems are equipped with ACAS Xu. Figure 4 shows a scenario where only AC2 is equipped and encounters AC1 at an angle of 90 deg, where both aircraft have the same speed and the RP has a slow response. In the graphs, dark colours represent the planned trajectories and light colours represent the achieved trajectories. In an attempt to follow the RWC guidance, AC2 turns left and right in a number of sequences and passes in front of AC1 at a distance of 1.9 km and an AFD of 4.5 km. Basically what happens is that the RWC bands suggest a turn away from the intruder, then after a while the RWC bands suggest that it is fine to turn right again and the RP does so to regain its original heading, this then induces again the RWC bands suggesting to turn left.

While in above example AC2 manages to pass AC1 and resolve the conflict situation, Figure 5 illustrates a livelock condition, which occurs in the same conditions except for a smaller relative heading of 45 deg. Here manoeuvring in accordance with the RWC guidance leads to AC2 being pushed away by AC1 enduringly. As a result, at the end of the simulation the AFD is 15.5 km in this example.

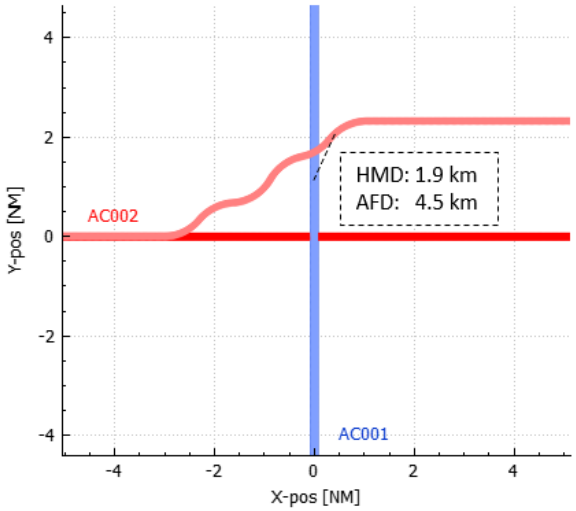

Figure 4. Deterministic simulation run: Xu DAA partial, slow RP, no sensor errors, 90 deg encounter, same speed

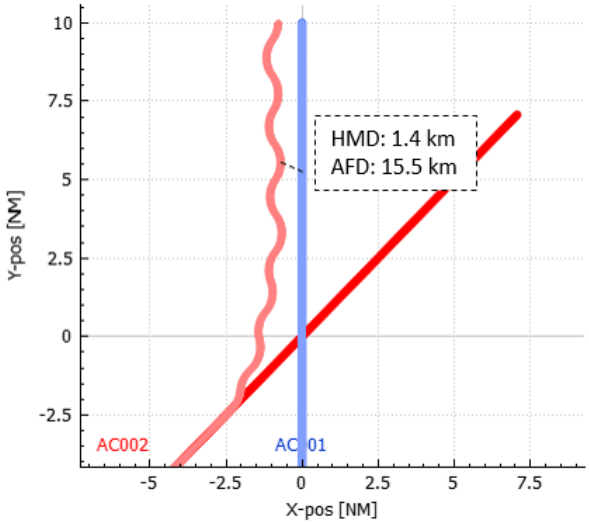

Figure 5. Deterministic simulation run: Xu DAA partial, slow RP, no sensor errors, 45 deg encounter, same speed

The dynamics of the ACAS Xu supported RPAS in an encounter depend on the realizations of the sensor errors and RP performance. As a result, various types of patterns can arise. Often livelock conditions similar to the one in Figure 5 are attained. However, another kind of a realization of the stochastic model is shown in Figure 6. Here AC2 turns right towards AC1 and it passes AC1 from behind. Although there is a LODW in this example, the AFD is limited to 3.6 km and it is a more effective solution than the one of Figure 5.

Also in encounter-scenarios where both RPAS are equipped with ACAS Xu and the RPs respond to the RWC guidance, livelock conditions can exist as illustrated in Figure 7. In this case, the combined effect of the RWC bands and RP response leads to both aircraft attaining fluctuating trajectories with an overall course that is about the mean of the planned courses of the aircraft.

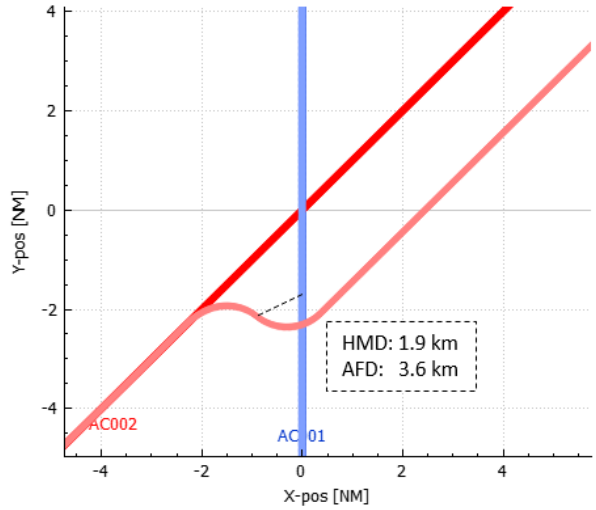

Figure 6. MC simulation run: Xu DAA partial, stochastic RP, with sensor errors, 45 deg encounter, same speed

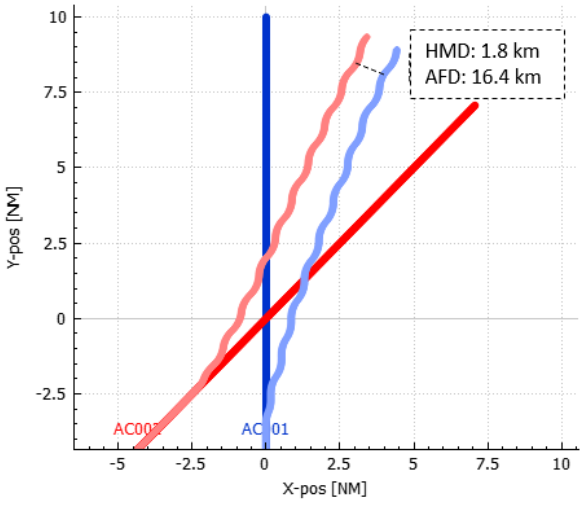

Figure 7. MC simulation run: Xu DAA full, stochastic RP, no sensor errors, 45 deg encounter, same speed

B. *A* DAA simulation runs for two-aircraft encounters*

Next, illustrative simulation results are shown for the cases where one or both of the RPAS use the A* DAA. Figures 8 and 9 show the trajectories of deterministic simulation runs, where only AC2 follows a DAA advised course with a slow RP for encounter angles of 90 and 45 degrees, respectively. These represent the same encounter-scenarios as shown in Figures 4 and 5 for ACAS Xu. The A* RWC guidance leads in both encounters to a right turn of AC2 towards AC1, such that AC2 passes behind AC1 at a distance of 2.2 to 2.3 km. No LODW is attained in these manoeuvres. The AFD over the simulated encounters is limited to 0.97 and 1.8 km. These additional distances are much smaller than those obtained in the ACAS Xu encounters, since the intruder is passed effectively without unduly heading fluctuations.

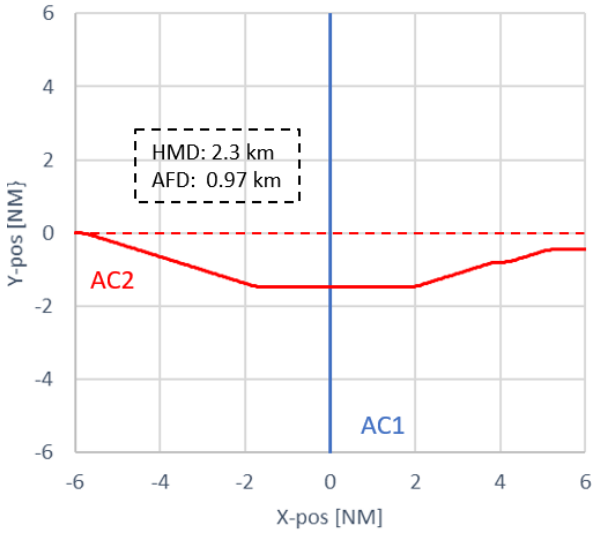

Figure 8. Deterministic simulation run: A* DAA partial or full, slow response, no sensor errors, 90 deg encounter, same speed

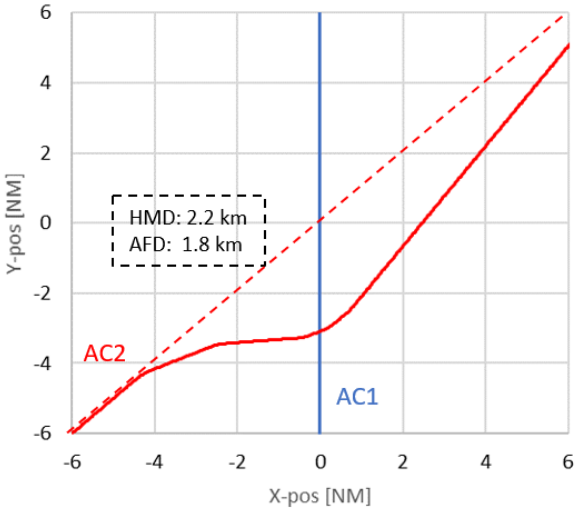

Figure 9. Deterministic simulation run: A* DAA partial or full, slow response, no sensor errors, 45 deg encounter, same speed

In the case that both RPAS use the A* DAA the results of the deterministic simulations are exactly the same as those for the scenarios where only AC2 is DAA equipped. As a result of the A* DAA setting, where AC2 is set as the first to adapt its route, the route of AC1 does not need to be changed, thus respecting its right-of-way. Also the impact of sensor errors and RP performance variability on the attained trajectories is small.

C. *Performance metrics for ACAS Xu and A* DAA two-aircraft encounters*

Statistics of the performance metrics for ACAS Xu and A* DAA over the encounter sets for the various scenarios are presented in Tables I and II. The results in Table I are for deterministic simulations, meaning that these are statistics over eight encounters. The results for ACAS Xu in these deterministic simulations show that LDWC conditions are frequently attained for the various scenarios, and in one run an NMAC condition is achieved. No LDWC or NMAC conditions are attained for the A* DAA. The attained mean HMD ranges from 1.9 km to 2.4 km for ACAS Xu, being larger if both RPAS are DAA equipped, while it is consistently 2.1 km for A* DAA. Regarding the AFD large differences exist between the A* DAA and ACAS Xu. Overall for A* DAA, the mean AFD is 945 m and the SD over the encounter-scenarios is 369 m; the differences between the scenarios are very small. In contrast for ACAS Xu, the overall mean AFD is 8.0 km and the overall SD is 8.4 km. The large values are indicative of the livelock conditions that exist for some of the encounters. The results show that the AFDs are larger if both aircraft are DAA equipped.

The statistics in Table II are for MC simulation of encounter-scenarios, where there can be sensor errors, RP performance variability, or both. Each encounter-scenario in a set is simulated in 100 runs, meaning that the statistics for each encounter-scenario are over 800 runs. The results for ACAS Xu show that for this set of encounters the LDWC percentage is increased considerably due to the stochastic factors. Overall LDWC occurred in 24.7% of the MC simulation runs versus in 12.5% of the deterministic simulation runs. The LDWC percentages are considerably higher for scenarios where only one aircraft is DAA equipped. The sensor errors also induce some NMACs in ACAS Xu scenarios that are without NMAC in the deterministic runs. In the A* DAA scenarios no LDWC or NMAC conditions occurred the simulations, meaning the A* DAA is robust for the considered sensor error and RP performance variability. The overall statistics for the HMD are similar for the deterministic and stochastic models, where the overall mean HMD remains 2.1 km for both ACAS Xu and A* DAA. The AFD is only minimally affected by the stochastic factors in the A* DAA scenarios, the overall mean is still about 950 m and the SD increased with 50 m to about 420 m. In the ACAS Xu scenarios larger increases in the mean and especially the SD can be observed. These large AFDs indicate that also in these stochastic scenarios, livelock conditions often occur.

As for the computational efficiency of the approaches, the durations of sets of simulations were tracked for computation on a Windows PC with Intel i5 Gen-11@2.60GHz processor. Each MC simulation run encompassed 10 minutes of flying time. On average the A* DAA MC simulation runs lasted 0.053 s per run. Each run includes at least one (partially equipped) or two (fully equipped) A* planning phases, while in the case of route adherence failures, there are more A* (re)planning phases. Such route adherence failures occurred mostly in the "slow" scenarios, where the closed loop delay was 12 s. For the ACAS Xu MC simulation runs, the mean time of an ACAS Xu simulation run lasted 0.094 s per run. Each run includes a call to ACAS Xu for one or two aircraft at each simulated second (i.e. 600 to 1200 times per run). So the call to ACAS Xu, due to its off-line optimization, is considerably quicker than the call to the A* DAA system, which uses an on-line optimization strategy. Nevertheless, the computation time of the A* DAA, which may be further improved by code optimization, is sufficiently small to support its application in operations.

TABLE I. STATISTICS OF SIMULATION OF DETERMINISTIC SCENARIOS OF TWO-AIRCRAFT ENCOUNTER SETS

Scenario					**Results**					
#	*Closed-loop delay*	*Sensor errors*	*DAA equipped*	*DAA type*	*LDWC (%)*	*NMAC (%)*	*HMD (m)*		*AFD (m)*	
							mean	*SD*	*mean*	*SD*
1	auto	no	partial	Xu	12.50%	0.000%	1905	162	4767	4605
				A*	0.00%	0.000%	2093	234	940	358
2	quick	no	partial	Xu	12.50%	0.000%	1923	173	4920	4603
				A*	0.00%	0.000%	2085	227	940	358
3	slow	no	partial	Xu	12.50%	0.000%	2048	330	5974	4496
				A*	0.00%	0.000%	2070	214	954	390
4	auto	no	full	Xu	12.50%	0.000%	2357	267	12564	11847
				A*	0.00%	0.000%	2093	234	940	358
5	quick	no	full	Xu	0.00%	0.000%	2183	117	12474	12026
				A*	0.00%	0.000%	2085	227	940	358
6	slow	no	full	Xu	25.00%	12.5%	2292	1071	7544	2854
				A*	0.00%	0.000%	2070	214	954	390
Combined results				Xu	12.50%	2.08%	2118	513	8041	8375
				A*	0.00%	0.000%	2083	225	945	369

TABLE II. STATISTICS OF MC SIMULATION OF STOCHASTIC SCENARIOS OF TWO-AIRCRAFT ENCOUNTER SETS

Scenario					Results					
#	*Closed loop delay*	*Sensor errors*	*DAA equipped*	*DAA type*	*LDWC (%)*	*NMAC (%)*	*HMD (m)*		*AFD (m)*	
							mean	*SD*	*mean*	*SD*
7	auto	yes	partial	Xu	27.00%	0.000%	2024	492	4979	4691
				A*	0.00%	0.000%	2123	236	910	389
8	quick	yes	partial	Xu	29.25%	0.000%	2036	536	5300	4806
				A*	0.00%	0.000%	2120	227	910	390
9	slow	yes	partial	Xu	50.63%	0.250%	1861	666	6244	5036
				A*	0.00%	0.000%	2132	229	956	476
10	auto	yes	full	Xu	13.50%	0.125%	2235	476	12898	14352
				A*	0.00%	0.000%	2185	283	959	414
11	quick	yes	full	Xu	14.75%	0.375%	2196	526	12190	12873
				A*	0.00%	0.000%	2181	279	959	414
12	slow	yes	full	Xu	38.00%	0.375%	2134	729	10207	9376
				A*	0.00%	0.000%	2191	283	1012	517
13	stoch.	no	partial	Xu	15.00%	0.000%	1935	180	4971	4629
				A*	0.00%	0.000%	2084	226	941	362
14	stoch.	no	full	Xu	10.63%	0.250%	2123	257	11227	13894
				A*	0.00%	0.000%	2084	226	941	362
15	stoch.	yes	partial	Xu	31.25%	0.000%	1996	533	5289	4822
				A*	0.00%	0.000%	2112	221	910	390
16	stoch.	yes	full	Xu	16.50%	0.125%	2183	526	11981	12826
				A*	0.00%	0.000%	2184	280	962	423
Combined results				Xu	24.65%	0.15%	2072	529	8529	10189
				A*	0.00%	0.000%	2140	254	946	417

D. Results for three-aircraft encounters

Although DAA systems are evaluated predominantly for aircraft pairs, also the performance for larger encounters is of interest. Figures 10 and 11 show illustrative simulation results for three-aircraft encounter-scenarios, where the aircraft are equipped with ACAS Xu or A* DAA, respectively. In the ACAS Xu encounter-scenario (Figure 10) the aircraft remain at sufficient distant without invoking a LDWC, but AC2 and AC3 do not attain their destination due to the interacting RWC guidance of these non-coordinating DAA systems.

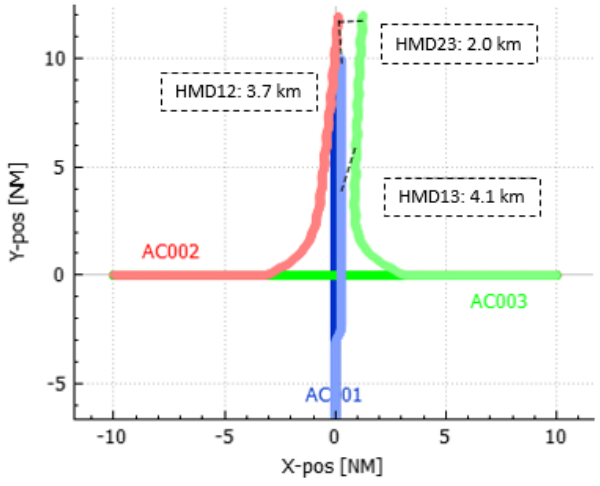

Figure 10. Deterministic simulation run for three ACAS Xu equipped aircraft with same speed, quick response, no sensor errors, headings 0, 90, 270 deg

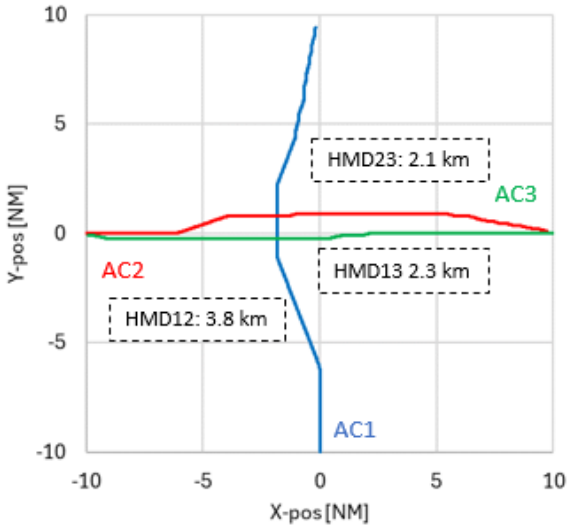

Figure 11. Deterministic simulation run for three A* DAA equipped aircraft with same speed, quick response, no sensor errors, headings 0, 90, 270 deg

In the A* DAA encounter-scenario (Figure 11) all aircraft reach their destination with a smallest HMD of 2.1 km and a total AFD of 1.9 km. It can be recognized that the sizes of the deviation from the shortest routes follow the order of the optimization sequence (AC1, AC2, AC3).

MC simulation was done for the most demanding A* DAA scenario, with stochastic delays and sensor noise (scenario 16). The set of 400 simulation runs for these encounter-scenarios do

not contain LDWC conditions or NMACs. The minimum HMD of the aircraft pairs is 2091 m on average (SD is 129 m). The AFD is 1421 m on average (SD is 180 m), i.e. 474 m per aircraft. These average HMD and AFD per aircraft are similar to the values obtained for the two-aircraft encounters. Each MC simulation run for the three aircraft lasted 0.129 s per run on the indicated Windows PC. This represents a more than linear increase with respect to the two-aircraft encounters, but is still sufficiently small for application in operations.

V. DISCUSSION

The development of effectively functioning DAA systems is a crucial step for the safe integration of RPA flights in a variety of airspace classes and in interaction with different airspace users. In the light of the three-layered conflict management processes (1) strategic conflict management, (2) separation provision or RWC, and (3) collision avoidance, a DAA system contributes to both the second and third layer [1]. While with the development and operational use of TCAS II there exists considerable experience and trust in the effectiveness of the 1-DOF (vertical) CA functionality of ACAS for manned flights, the development and validation of the multi-DOF CA and RWC functionalities of DAA systems for RPAS is considerably more complicated.

Given the close connection of DAA systems with ACAS it is no surprise that their development has built to a considerable extent on system architectures and algorithms of ACAS. For instance, the types of rules applied in DAIDALUS have been inspired by TCAS II algorithms [3], and the TRM of ACAS Xu is largely based on the same type of DP optimization as ACAS Xa [5, 14]. Also the types of input data of DAA systems are similar to those employed by ACAS, both using state data for the (relative) position and speed of the aircraft in an encounter.

By simulations of a stochastic dynamic agent-based model of sociotechnical RPAS pairs, both equipped with ACAS Xu [13], it was found earlier [8] that livelock conditions exist, such that the flights do not manage to effectively pass each other. The examples and statistics in the current paper show that such livelock conditions also exist if only one of the aircraft manoeuvres in line with the RWC guidance by ACAS Xu and the other just flies straight ahead (because it has right-of-way or does not have a DAA system). The livelock condition exists because the RP is assumed to return to its planned course if allowed so by the RWC bands and then comes into conflict with the other RPAS. Such livelock conditions were not found in HITL simulations for ACAS Xu [15]. However, LDWC attributions by RPs like “pilot attempting to return to the route too soon following an avoidance manoeuvre” were found in the HITL experiments, and such manoeuvring is similar to the modelled RP performance in a livelock. In general, the oversight of RPs over the traffic situation may help to avoid or overcome livelock conditions. Nevertheless, the fact that strictly following the RWC bands of ACAS Xu can induce livelock conditions in a range of encounter geometries, is a clear weakness of the RWC function of ACAS Xu.

This type of performance indicates a limitation in the scope of current DAA systems [2-6]. They only provide guidance on how to avoid other traffic, but they do not provide guidance on how to regain the route to the desired destination without inducing new conflicts. This is a distinction with the separation provision by air traffic controllers, who provide instruction for separation as well as for getting back on the planned route, based on their awareness of both the positions and planned routes of the involved traffic. The intent-based DAA approach proposed in this paper implies that the same types of traffic information (state and intent) are used by both ATC and DAA system in the second layer of conflict management. Also the way that intent-based DAA system processes the information and comes to RWC guidance has similarity with ATC processes. In particular, the intent-based DAA system uses a central agent that plans routes for all involved aircraft based on knowledge of the states and intents of the aircraft. The central agent can be one of the aircraft involved in the encounter, which has been agreed by the other aircraft to adapt the routes of all aircraft to remain well clear. Such central agent aircraft should have the technical capability to provide a timely solution. For cases where multiple aircraft are capable of serving this role, there should be a leader selection process, e.g. like the rule used in ACAS II that provides priority to aircraft with the lowest Mode S address in the case of simultaneous RAs. The central agent can also be a ground-based station like an ATC centre or a UAS service provider, as an automated function for separation provision.

The conflict resolution approach applied in the intent-based DAA system extends the A* path planning approach of [9]. Innovations with respect to that work concern the following. While in [9] only uncertainty in the positions of intruders was incorporated, our approach considers uncertainty contributions of ownship and intruder for the conflict risk cost function. Furthermore, the notion of infinite costs below a particular safe separation distance in [9] has been discarded, as it is not needed to attain sufficient separation. Most importantly, different path cost and heuristic functions (Eq.(9)) are used in our approach. Herein we have included aircraft specific flight trajectory element costs, which allows to specify priorities between aircraft. Also, we have incorporated a heuristic function that uses the distance to the final waypoint, which can assure that the heuristic function is admissible and therefore the A* search is cost-optimal.

The achieved results show that the A* DAA system provides effective RWC guidance without any LDWC or NMAC conditions and limited AFDs. The A* DAA system is robust for sensor errors, variation in closed-loop delays, and scenarios with one or both RPA being equipped. These results are in contrast with those attained for ACAS Xu, where LDWC and NMAC conditions were found, as well as large AFDs due to the livelock phenomenon. Furthermore, the ACAS Xu sociotechnical RPAS was found to be sensitive for sensor errors and closed-loop delays, which can trigger large changes in the aircraft trajectories. When looking at individual realizations of the ACAS Xu and A* DAA based simulations, two main differences can be recognized. Firstly, the A* DAA system initiates its RWC guidance earlier, at about 190 s rather than at about 100 s before the original CPA. Secondly, the A* DAA system turns one of the aircraft towards the other aircraft, while ACAS Xu typically turns it away. In combination, the A* DAA guidance thus steers one of the aircraft to pass behind

and avoids ending up in a livelock. On average, the attained HMDs are about 2100 m for both ACAS Xu and the A* DAA. For ACAS Xu, the timing of the guidance and the achieved HMDs depend on the look-up tables, such as determined in the off-line DP optimization, and the RWC roll-out approach. For the A* DAA, they depend on its optimization settings, such as the size of the prediction errors and the tuning constants in the cost function. As such the timing and achieved separation can be adapted to accommodate particular airspace requirements.

The POMDP-based dynamic programming applied in ACAS Xu is a single-agent optimization method focused on maintaining sufficient distance with an intruder, assuming a constant course of the intruder and no coordination. The A* DAA approach is a multi-agent optimization method focused on maintaining sufficient distance and reaching destination, by coordinating with intruders that share planned routes. The multi-agent optimization problem is solved by a series of local optimizations for the aircraft in the encounter, where the path of one aircraft is adapted while the other paths are fixed. This means that it does not use an overall global criterion for the multi-agent optimization and it implies that the attained solution depends on the ordering of the aircraft in the optimization sequence. The results shown indicate that the ordering can be used as a means of prioritisation, such that aircraft early in the sequence deviate more from their shortest route. In general though, more research is needed regarding the impact of the optimization parameters and sequence order in a wide variety of encounter-scenarios. Such knowledge enables to adapt the optimization approach towards operationally acceptable results, which can be validated in enhanced fast-time simulation, human-in-the-loop simulation and real-world testing.

In general, multi-agent optimization problems are hard and they can scale poorly with the number of involved agents [16]. The results in this paper show that the computation time of the A* DAA approach is sufficiently low for encounters with small numbers of aircraft. This is well in line with the custom focus on two-aircraft encounters for the development of DAA systems [2-6]. However, the computational load may become excessive for optimization of many trajectories in dense airspace. The computational complexity for such cases should be studied, and evaluated taking into consideration the likelihood of multi-aircraft encounters in operational environments.

In conclusion, the intent-based A* DAA approach was shown to function effectively for sets of encounter-scenarios that are problematic for the state-based ACAS Xu system. As such, the A* DAA system is a promising approach for a more effective DAA. In future work the effectiveness of the A* DAA approach will be further analysed for more complicated encounter-scenarios.

REFERENCES

[1] ICAO, "Manual on Remotely Piloted Aircraft Systems (RPAS)," International Civil Aviation Organization, Montréal, Canada, Doc 10019, 2015.

[2] RTCA, "Minimum Operational Performance Standards (MOPS) for Detect and Avoid (DAA) Systems," DO-365B, 18 March 2021.

[3] C. Munoz *et al.*, "DAIDALUS: Detect and Avoid Alerting Logic for Unmanned Systems," presented at the Proceedings of the 34th Digital Avionics Systems Conference (DASC 2015), Prague, Czech Republic, 2015.

[4] EUROCAE, "Minimum Aviation System Performance Standards for Detect And Avoid (Traffic) for Remotely Piloted Aircraft Systems in Airspace Classes A-C under IFR," ED-271A, November 2024.

[5] M. P. Owen, A. Panken, R. Moss, L. Alvarez, and C. Leeper, "ACAS Xu: Integrated collision avoidance and detect and avoid capability for UAS," presented at the 2019 IEEE/AIAA 38th Digital Avionics Systems Conference (DASC), 2019.

[6] EUROCAE, "Minimum operational performance standards for Airborne Collision Avoidance System Xu (ACAS Xu): Volume I," ED-275, December 2020.

[7] D. P. Bertsekas, "Rollout algorithms for discrete optimization: A survey," in *Handbook of combinatorial optimization*, vol. 5: Springer New York, 2013, pp. 2989-3013.

[8] S. Stroeve, C. J. Villanueva Cañizares, and G. Dean, "The critical impact of remote pilot modelling in evaluation of detect-and-avoid systems explained for ACAS Xu," *European Journal of Transport and Infrastructure Research*, vol. 24, no. 4, pp. 1-17, 2024, doi: https://doi.org/10.59490/ejtir.2024.24.4.7380.

[9] P. Zhao, H. Erzberger, and Y. Liu, "Multiple-Aircraft-Conflict Resolution Under Uncertainties," *Journal of Guidance, Control, and Dynamics*, vol. 44, pp. 1-19, 09/06 2021, doi: 10.2514/1.G005825.

[10] S. Russell and P. Norvig, *Artificial Intelligence: A Modern Approach*, Fourth edition ed. Pearson, 2021.

[11] S. H. Stroeve and C. J. Villanueva Cañizares, "CAVEAT TAM - Models and Algorithms: Development of a Collision Avoidance Evaluation and Analysis Tool," Royal Netherlands Aerospace Centre NLR, Amsterdam, The Netherlands, NLR-CR-2023-285, August 2023.

[12] S. H. Stroeve, H. A. P. Blom, C. H. Medel, C. G. Daroca, A. A. Cebeira, and S. Drozdowski, "Modeling and simulation of intrinsic uncertainties in validation of collision avoidance systems," *Journal of Air Transportation*, vol. 28, no. 4, pp. 173-183, 2020, doi: 10.2514/1.d0187.

[13] EUROCAE, "Minimum operational performance standards for Airborne Collision Avoidance System Xu (ACAS Xu): Volume II Algorithm Design Description," ED-275, December 2020.

[14] M. J. Kochenderfer, J. E. Holland, and J. P. Chryssanthacopoulos, "Next-generation airborne collision avoidance system," *Lincoln Laboratory Journal*, vol. 19, no. 1, pp. 17-33, 2012.

[15] R. C. Rorie, C. Smith, G. Sadler, K. J. Monk, T. L. Tyson, and J. Keeler, "A Human-in-the-Loop Evaluation of ACAS Xu," presented at the 2020 AIAA/IEEE 39th Digital Avionics Systems Conference (DASC), 11-15 Oct. 2020.

[16] J. Cerquides, A. Farinelli, P. Meseguer, and S. D. Ramchurn, "A Tutorial on Optimization for Multi-Agent Systems," *The Computer Journal*, vol. 57, no. 6, pp. 799-824, 2014, doi: 10.1093/comjnl/bxt146.